Impurity centers in $PbTiO_3$ single crystals: An electron-spin-resonance analysis

V. V. Laguta, M. D. Glinchuk, I. P. Bykov, and Yu. L. Maksimenko
Institute for Problem of Material Sciences, Ukrainian Academy of Science, Krgiganovskogo 3, 252180 Kiev, Ukraine

J. Rosa and L. Jastrabík
Institute of Physics, Academy of Sciences of the Czech Republic, Cukrovarnická 10, 16200 Prague, Czech Republic
(Received 15 January 1996; revised manuscript received 15 April 1996)

Impurities in a nominally undoped *c*-domain $PbTiO_3$ single crystal have been studied by ESR in a wide temperature interval (4.2–700) K before and after light illumination. Several 3*d*-metal paramagnetic impurities substituting for Ti^{4+} (Mn^{4+}, Fe^{3+}, and Ni^{3+}), as well as light-induced centers (Pt^{3+}, Ti^{3+}-V_O-*A* [Pb] and Ti^{3+}-*A* [Pb]) were revealed in the crystal. A comparison of the observed temperature dependence of the axial crystal field constant with a calculation based on a Newman model allows one to show that Mn^{4+} occupies an off-center position in the oxygen cage similarly to Ti^{4+}, while Fe^{3+} remains centered at any temperature, its excess charge being compensated in the distant spheres. The temperature dependence of Ti^{4+} ion displacements obtained on the basis of ESR data analysis is in good agreement with neutron diffraction measurements and does not confirm recent x-ray-absorption fine-structure data on the Ti^{4+} off-center position at $T>T_c$. The Ni^{3+} center and the light-induced titanium centers have not been considered previously. The Ti^{3+}-V_O-*A* [Pb] center models can be imaged as an electron on a titanium ion nearest to the oxygen vacancy and a defect on a neighboring Pb site (F_A-center model). It has been shown that Pt^{3+} and Ti^{3+}-V_O-*A* [Pb] are shallow donors based on an analysis of the temperature dependence of their ESR intensities. [S0163-1829(96)00741-2]

I. INTRODUCTION

Lead titanate is a model crystal of the perovskite family which has been considered as a displacive-type ferroelectric. At $T_c = 763$ K $PbTiO_3$ goes through a weak first-order transition from the paraelectric cubic to the ferroelectric tetragonal phase. It was shown[1] that both Pb and Ti atoms are displaced from their respective oxygen planes by 0.047 and 0.03 nm at $T=300$ K, the ratio of lattice constants being $c/a=1.06$. Contrary to $BaTiO_3$ the oxygen octahedron is not distorted during this phase transition. A schematic representation of ferroelectric phase symmetry is shown in Fig. 1. In spite of the simplicity of the $PbTiO_3$ structure its investigation has been continued up to now, e.g., some indication of local distortions at $T>T_c$ supporting an order-disorder mechanism for the phase transition was obtained by x-ray-absorption-fine structure (XAFS).[2] Difficulties in growing high quality $PbTiO_3$ single crystals and the extensive application of $PbTiO_3$ ceramic material, resulted in a preference for ceramic samples in many works. This makes it cumbersome to clear up problems concerning $PbTiO_3$ structure and properties including the strong influence of impurities and lattice defects. Many impurities, e.g., Fe, Ni, and Mn are present even in nominally pure high quality single crystals of $KTaO_3$ (Ref. 3) and $BaTiO_3$ (Ref. 4). On the other hand, several metastable lattice defects, such as vacancies, trapped electrons or holes, etc., may be the consequence of technology or material treatment. Up to now, however, the number of publications on the impurities and defects in $PbTiO_3$ is still small. The iron impurities are most frequently studied by ESR.[5–7] Two Fe^{3+} ESR spectra of axial symmetry with axial crystalline field parameters $b_2^0=1.187$ cm^{-1} and 1.150 cm^{-1} at $T=77$ K were observed in a $PbTiO_3$ single crystal doped with iron.[6] ESR lines were very broad with a width of about 10 mT and 30 mT for the first and the second spectrum, respectively. Since Fe^{3+} substitutes for Ti^{4+} it was assumed that the spectrum with larger b_2^0 was due to a $Fe^{3+}(Ti^{4+})$-V_O center (V_O denoting an oxygen vacancy in the nearest neighbor position required for excess charge compensation) while the axial character of the second spectrum was attributed to ferroelectric distortion. Two axial Fe^{3+} ESR spectra were also observed at room temperature in nominally pure $PbTiO_3$ crystals, their crystal field constants being $b_2^0=0.503$ cm^{-1} and 0.9 cm^{-1} (see Ref. 7). The observed linewidths were as broad as those mentioned above. This gives evidence of the low quality of the investigated single crystals. The observation of Mn^{4+}, Mn^{2+}, Cr^{3+}, and Cr^{5+} paramagnetic centers in $PbTiO_3$ ceramic samples doped with MnO (Ref. 8) and Cr_2O_3 (Ref. 9) should also be noted. The ESR parameters of all these ions (*g* factors and b_2^0) were measured in the temperature region (4.2–800) K.

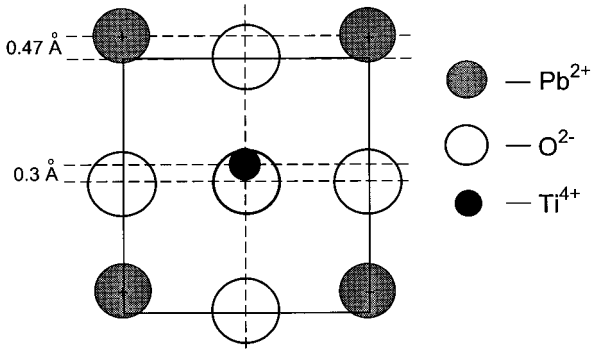

FIG. 1. Schematic representation of ionic displacements in $PbTiO_3$ ferroelectric phase.

TABLE I. ESR spectral parameters of d transition-metal impurities in $PbTiO_3$.

Ion	T (K)	g	b_l^m (cm^{-1})	A (10^{-4} cm^{-1})	A^{Pb} ($10^{-4}cm^{-1}$)
Mn^{4+}	290	$g_\parallel$: 1.997(2)	b_2^0: 0.3157(5)	$A_\parallel$: 78(1)	$A_\perp$: 7.4(1)
		$g_\perp$: 1.985(1)		$A_\perp$: 70.4(2)	
Fe^{3+}	290	$g_\parallel$: 2.009(5)	b_2^0: 0.905(4)		$A_\parallel$: 1.2(1)
		$g_\perp$: 2.010(5)	b_4^0: -0.0035(40)		
			b_4^4: 0.1400(70)		
Ni^{3+}	77	$g_\parallel$: 2.0128(2)			$A_\parallel$: 9.3(2)
		$g_\perp$: 2.4819(2)			$A_\perp$: 8.1(2)
Pt^{3+} [a]	35	$g_\parallel$: 1.9316(4)		$A_\parallel$: 166(2)	$A_\parallel$: 2.3(2)
		$g_\perp$: 2.4752(6)		$A_\perp$: 324(1)	$A_\perp$: 4.0(2)

[a]Annealed at 100 K.

The study of Mn^{4+} ESR spectra in $PbTiO_3$:Mn single crystals at room temperature was performed in Ref. 10. The ESR spectrum of Pt^{3+} which appeared in $PbTiO_3$ after light illumination has been recorded recently in Ref. 11.

It is seen that the available information about impurities in $PbTiO_3$ is very poor and contradictory because it has been obtained on low quality single crystals and ceramic samples. Besides, the proposed impurity center models are not based on any quantitative consideration and have to be rechecked.

In this work we carried out the study of ESR spectra of a nominally pure $PbTiO_3$ single crystal of high quality. As a result all the observed ESR lines are very narrow (less than several G) and hyperfine as well as superhyperfine structures were perfectly resolved. We discovered and identified Fe^{3+}, Mn^{4+}, Ni^{3+}, Pt^{3+}, Ti^{3+}-V_O-A [Pb] and Ti^{3+}-A [Pb] as paramagnetic centers, the last four of these centers were induced by light. The measurements were carried out in a wide temperature interval (4.2–700) K which made it possible to find out the structure of paramagnetic centers by a comparison of observed and calculated crystal field constants within the framework of the Newman model. It was shown that Pt^{3+} and Ti^{3+}-V_O-A [Pb] are shallow donors in the crystal band gap.

II. THE SAMPLES AND EXPERIMENTAL DETAILS

The samples were grown by cooling the B_2O_3–PbO melt containing stoichiometric amounts of $PbCO_3$ and TiO_2. The crystals were made single domain, using the effect of unaxial mechanical compression. The domain structure was checked by a polarizing microscope.

The ESR spectra were recorded in the X-wave region at $4.2<T<700$ K. The Oxford Instruments ESR-9 cryosystem was used. High temperatures ($T>300$ K) were obtained by passing a current of warm nitrogen gas over the sample.

An arc lamp (200 W) equipped with a set of optical filters (wavelengths 365, 405, 436, 546, and 577 nm) was applied for optical irradiation of the samples in a resonator. The duration of illumination was about 2 min. The temperature region of the paramagnetic center's stability was obtained by heating up the sample to a definite T with subsequent recording of the ESR spectrum at low temperature.

III. EXPERIMENTAL RESULTS AND THEIR DESCRIPTION

We have investigated $PbTiO_3$ single crystals with c domains only, the portion of other domain types was negligibly small. Therefore, all ESR spectra of the paramagnetic centers had at least axial symmetry with the axis along the c direction.

The desirable information about the position, charge state, local symmetry, etc. of impurities is usually obtained by the use of a spin Hamiltonian. The spectra are generally described by the spin Hamiltonian of type

$$\hat{\mathcal{H}}=\beta\hat{\mathbf{S}}\cdot\mathbf{g}\cdot\mathbf{B}+\frac{1}{3}(b_2^0O_2^0+b_2^2O_2^2)+\frac{1}{60}(b_4^0O_4^0+b_4^4O_4^4)$$
$$+\hat{\mathbf{S}}\cdot\mathbf{A}\cdot\hat{\mathbf{I}}+\sum_k\hat{\mathbf{S}}\cdot\mathbf{A}^k\cdot\hat{\mathbf{I}}^k, \quad (1)$$

allowing for the Zeeman, axial, and cubic crystal fields, hyperfine and superhyperfine interactions. Here $\hat{\mathbf{S}}$, $\hat{\mathbf{I}}$ are the electron and nuclear spins of the paramagnetic center, respectively, $\hat{\mathbf{I}}^k$ is the nuclear spin of the kth lattice ion and O_l^m are conventional electron spin polynomials. The parameters of the spin Hamiltonian can be found by fitting the angular dependence of the observed line positions with those calculated with the help of Eq. (1).

The obtained parameters of the spin Hamiltonian for all paramagnetic centers in nominally undoped $PbTiO_3$ single crystal observed in this work are listed in Tables I and II.

Let us proceed to a detailed analysis of the observed spectra and their description on the basis of spin Hamiltonian (1).

A. Mn^{4+} ($3d^3$, $S=3/2$)

The ESR spectrum of manganese ions can be readily identified because six hyperfine lines are characteristic of nuclear spin $I=5/2$, the value of hyperfine splitting being close to that in other materials with perovskite structure.[12,13] The observed angular dependence of Mn^{4+} ESR line positions (Fig. 2) was described by spin Hamiltonian (1) with the following parameters taken at $T=290$ K: $b_2^0=3157\times10^{-4}$ cm^{-1}, $g_\parallel=1.997$, and $g_\perp=1.985$. Only two transitions $(1/2\leftrightarrow-1/2)$ and $(3/2\leftrightarrow1/2)$ were observed in the X region because the b_2^0 value appeared to be rather large. For $\theta=90°$ ($\mathbf{B}\perp c$), where θ is the polar angle of the constant magnetic field $\mathbf{B}$, the ESR lines of the transition $(1/2\leftrightarrow-1/2)$ are very narrow, $\Delta B_{1/2,-1/2}=0.2$ mT (see the inset in Fig. 2). When the magnetic field is deflected from this direction the linewidths increase and at $\theta<20°$ the lines almost disappear. The lines of the $(1/2\leftrightarrow-1/2)$ transition be-

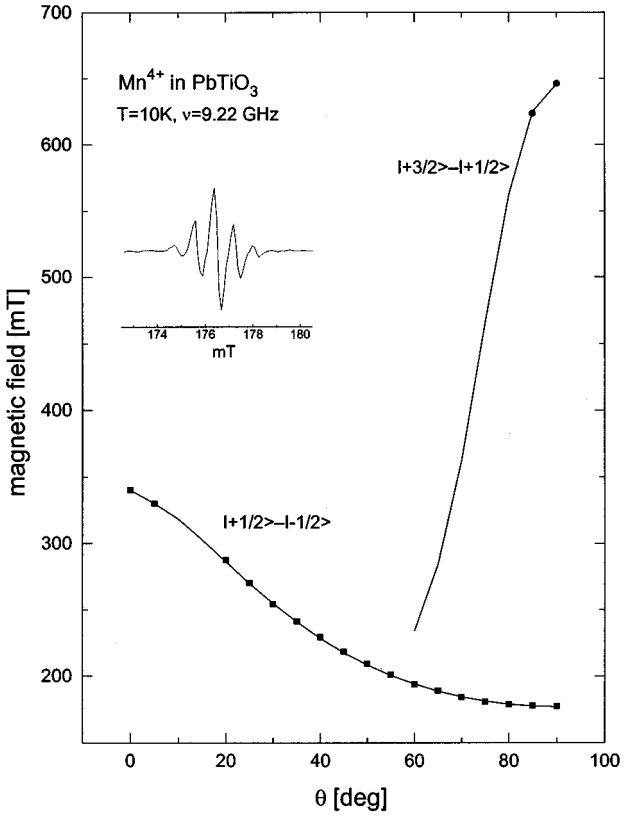

FIG. 2. The angular dependence of Mn^{4+} resonance fields in $PbTiO_3$ (solid lines, theory; points, experiments). The superhyperfine splitting of the ESR line is also shown.

come observable again only near $\theta = 0°$. Such a strong angular dependence of linewidths of the transition $(1/2 \leftrightarrow -1/2)$ may result from the crystal mosaic structure. In this case the ESR linewidth has to be proportional to $\delta B_r / \delta\theta$, where B_r is the resonance field at the line center.

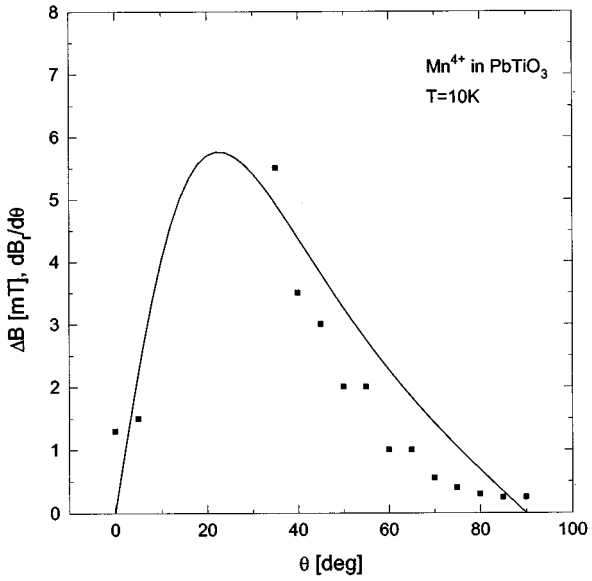

FIG. 3. The angular dependence of Mn^{4+} ESR linewidth ΔB (squares) and $\delta B_r / \delta\theta$ (solid line) in $PbTiO_3$.

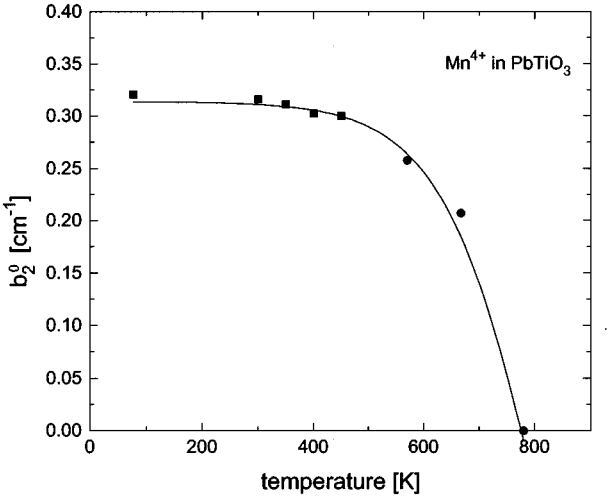

FIG. 4. The temperature dependence of b_2^0 for Mn^{4+}. Squares, our experimental data; circles, data after Ref. 8; solid line, theory.

The dependence of the linewidth $\Delta B_{1/2,-1/2}$ and $\delta B_r / \delta\theta$ on the magnetic field orientation is depicted in Fig. 3. The correlation between these values is obvious. However, the absence of a similar broadening for other paramagnetic centers, including axial Fe^{3+} contradicts the assumption of the crystal mosaic structure. It seems that Mn^{4+} impurities are distributed nonrandomly and prefer the regions with fluctuations of the c-axis orientation. These regions may be nearby crystal structure imperfections as well as nearby domain boundaries. With temperature increasing up to $T = 500$ K the lines broaden, but the common view of the spectrum is conserved.

Due to the same charge states of Mn^{4+} and Ti^{4+} and the similarity of their ionic radii one can reasonably assume that Mn^{4+} substitutes for Ti^{4+}. The well-resolved superhyperfine structure of Mn^{4+} at $T < 77$ K (Fig. 2) and the magnitude of superhyperfine splitting of 0.8 mT speak in favor of this supposition. Indeed, the x-ray measurements gave evidence of the fact that in the tetragonal phase of $PbTiO_3$ in any unit cell the distance between a titanium ion and four nearest and more distant lead ions equals to 0.334 nm and 0.356 nm, respectively. Keeping in mind exponential decreasing with distance of isotropic superhyperfine interaction one can assume that only four equivalent nearest lead ions give a resolved superhyperfine structure. Taking into consideration that the natural abundance of ^{207}Pb ($I = 1/2$) is 22.6%, we have calculated that the ratio of superhyperfine line intensities has to be 100:48:9, which is in a very good agreement with the observed ratio of 100:48:10. The details of Mn^{4+} behavior (whether Mn^{4+} is displaced in the same way as Ti^{4+} or stays in the oxygen cage center) may manifest itself in the observed temperature dependence of b_2^0 (see Fig. 4). Thus, the consideration of Mn^{4+} displacement at different temperatures may be relevant for the Ti^{4+} displacement and, hence, for the phase transition investigation itself. This problem will be discussed in more detail below in Sec. V.

B. Fe^{3+} ($3d^5$, $S = 5/2$)

In a wide temperature region we have observed another two-line spectrum which is more intense than that of

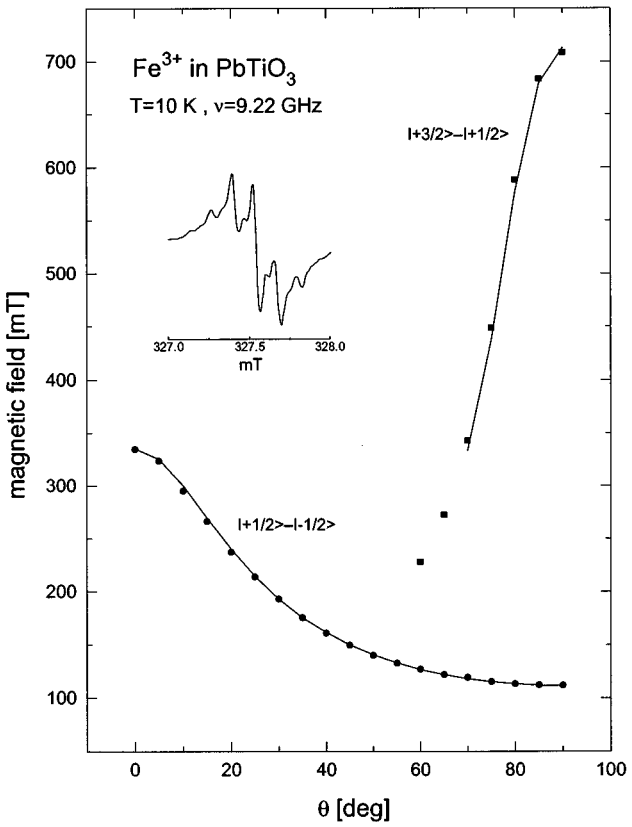

FIG. 5. The angular dependence of Fe^{3+} resonance fields in $PbTiO_3$ (solid lines, theory; points, experiment). The superhyperfine splitting of the ESR line is also shown.

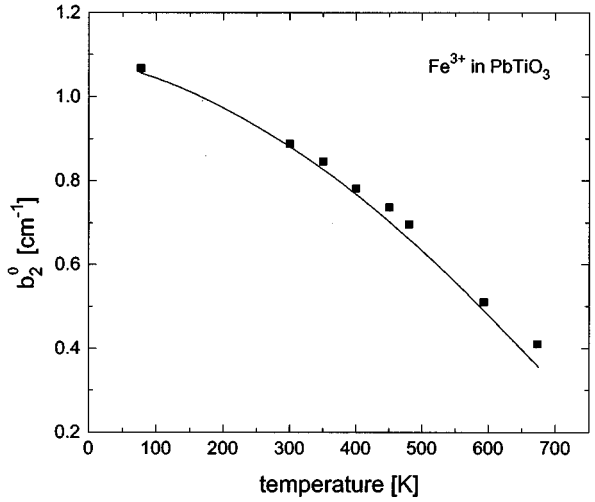

FIG. 6. The temperature dependence of b_2^0 for Fe^{3+} (squares, experiment; solid line, theory).

Mn^{4+}. The angular dependence of its resonance field shows the axial symmetry with the axis along the c axis of the crystal (see Fig. 5). The line positions were perfectly described by spin Hamiltonian (1) for a paramagnetic center with $S=5/2$ and the following parameters at $T=290$ K: $g_\parallel=2.009(5)$, $g_\perp=2.010(5)$, $b_2^0=0.905(4)$ cm^{-1}, $b_4^0=-0.0035(40)$ cm^{-1}, and $b_4^4=0.1400(70)$ cm^{-1}. At low temperatures ranging from 4.2 to 77 K a superhyperfine structure is observed on the line of the transition $(1/2\leftrightarrow -1/2)$ (see inset in Fig. 5) which resembles that in the Mn^{4+} spectrum. The lines are very narrow, $\Delta B=0.05$ mT at $T=10$ K. We assume that the observed spectrum belongs to Fe^{3+} substituted for Ti^{4+} on the basis of the following reasons: (i) it is well known that all titanium containing oxides always have the admixture of iron ions; (ii) the number of paramagnetic ions with $S=5/2$ and $I=0$ is strongly restricted (Fe^{3+} or Cr^{+} the latter having an isotope with $I=3/2$, its natural abundance being 9%); (iii) the observed superhyperfine structure shows that the paramagnetic ion has to substitute for Ti^{4+}. The ionic radii of Ti^{4+} and Fe^{3+} ions are close to one another ($R_{Ti^{4+}}=0.068$ nm, $R_{Fe^{3+}}=0.064$ nm) while $R_{Cr^{+}}=0.081$ nm, i.e., $R_{Cr^{+}}-R_{Ti^{4+}} \gg R_{Ti^{4+}}-R_{Fe^{3+}}$. The charge state of Fe^{3+} is also closer to that of Ti^{4+} than in the Cr^{+} case.

The comparison of our parameters with those of Fe^{3+} measured earlier[5–7] seems to be cumbersome because of their broader lines and parameter scattering which may be the consequence of low quality $PbTiO_3$ (see the Introduction). On the other hand, in the crystals doped with iron various paramagnetic centers may have appeared: $Fe^{3+}(Ti^{4+})$-V_O, $Fe^{3+}(Pb^{2+})$-V_{Pb}, $Fe^{3+}(Ti^{4+})$-$Fe^{3+}(Pb^{2+})$ pairs, etc. The number of these centers must have depended on the technology of crystal preparation and also on their subsequent treatment. Note that six different paramagnetic iron centers were discovered in $KTaO_3$ (see Refs. 14 and 15).

The extremely narrow lines of the Fe^{3+} ESR spectrum ($\Delta B\simeq 0.05$ mT at $T=10$ K) observed in this work made it possible to avoid any ambiguity in the spectrum interpretation in a wide temperature range. The analysis (see Sec. V) of the observed temperature dependence of b_2^0 (Fig. 6) shows that Fe^{3+} (Ti^{4+}) remains centered in its surrounding oxygen cage and that the Fe^{3+} excess charge compensation takes place in spheres distant from the paramagnetic center. $b_2^0(T)$ data were derived under the assumption that other spin Hamiltonian parameters have no temperature dependence, because we did not observe their change at $4.2\leqslant T\leqslant 300$ K, where detailed data on the angular dependence of ESR line positions were measured. On the other hand, the magnitudes of b_4^0 and b_4^4 are much smaller than the observed change of b_2^0 with temperature; thus, their variations at $T>300$ K (if any) can be neglected.

Note that a conclusion about a more centered position of Fe^{3+} in the oxygen cage in comparison with that of Mn^{4+} follows from a comparison of their linewidths: $\Delta B_{Fe}\ll\Delta B_{Mn}$ due to a more distant second set of Pb ions in the case of iron (see Fig. 1), because the superhyperfine interaction with the second set of ^{207}Pb nuclei contributes to the linewidth.

C. Ni^{3+} ($3d^7$, $S=1/2$)

At $4.2\leqslant T\leqslant 150$ K we have observed a one line ESR spectrum with a superhyperfine structure (Fig. 7). It was described by spin Hamiltonian (1) for a paramagnetic center with $S=1/2$ and the following parameters ($T=77$ K): $g_\parallel=2.0128(2)$, $g_\perp=2.4819(2)$. At $T>150$ K the linewidth strongly increases and at room temperature the line becomes

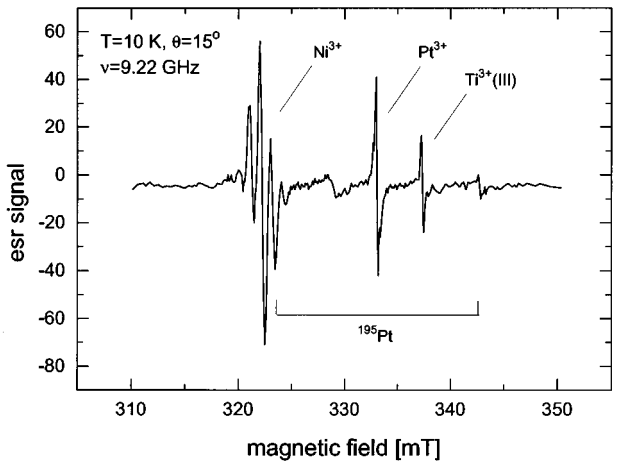

FIG. 7. ESR spectra of light-induced centers in $PbTiO_3$ after illumination.

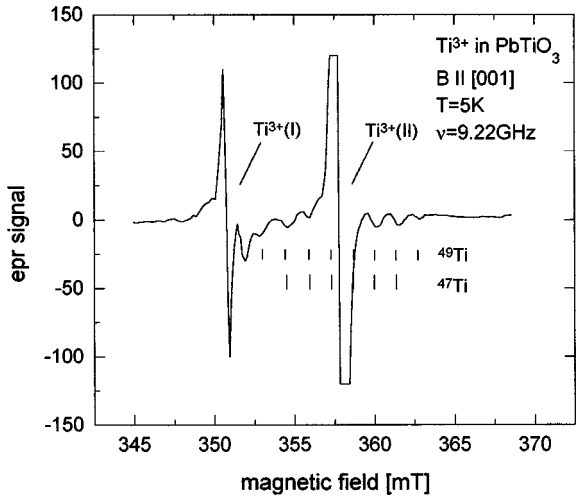

FIG. 8. ESR spectra of Ti^{3+}(I) and Ti^{3+}(II) (both assumed to be Ti^{3+}-V_O-*A* [Pb] centers) in $PbTiO_3$ after illumination.

invisible. The observed superhyperfine structure of the line looked like Mn^{4+} (Ti^{4+}) and Fe^{3+} (Ti^{4+}) which gave evidence of the fact that the paramagnetic center substituted for Ti^{4+}. We assume that this center is an Ni^{3+} ion on the basis of the following reasons. The values of g factors, namely, $g_\parallel$, $g_\perp > g_e$ (g_e is g factor of free electron), speak in favor of the fact that more than 1/2 of the electron shell has to be filled. Since $g_\parallel \approx g_e$, $g_\perp > g_e$ the ground orbital state has to be the d state, d_{z^2} being the lowest one. Indeed, in this case[16]

$$g_\parallel = g_e, \quad g_\perp = g_e - \frac{6\lambda}{\Delta}, \tag{2}$$

where λ is the value of spin-orbit coupling, Δ is the energy gap between the ground and the nearest excited state. Note that expressions (2) are valid for the case of the stretched oxygen octahedron corresponding to $PbTiO_3$ tetragonal phase structure. We did not observe any hyperfine structure, thus, the nuclear spin of the paramagnetic ion has to be zero (or its natural abundance has to be small). The paramagnetic centers which satisfy all of the aforementioned conditions are Ni^+ ($3d^9$, $S=1/2$), Fe^+ ($3d^7$, $S=1/2$), and Ni^{3+} ($3d^7$, $S=1/2$), the last two having $S=1/2$ in the low-spin state. Keeping in mind that Ni^{3+} is closer to Ti^{4+} both in the charge state and in the ionic radius value we prefer the Ni^{3+} ion. In the next section we shall continue the consideration of the peculiarities of the Ni^{3+} ESR spectrum because the spectrum appeared sensitive to light illumination.

IV. LIGHT-INDUCED PARAMAGNETIC CENTERS

After the illumination of the $PbTiO_3$ crystal by a light beam with $\lambda < 436$ nm at $T \approx 10$ K four new ESR spectra appear. The Ni^{3+} ESR spectrum intensity strongly increases, the Fe^{3+} and Mn^{4+} spectra remain unchanged. The new ESR spectra are represented in Figs. 7 and 8. One of the spectra exhibits axial symmetry, the angular dependence of its line positions is described by spin Hamiltonian (1) for $S=1/2$. This spectrum was identified as that of Pt^{3+} ($5d^7$) in strong crystalline field ($S=1/2$). The characteristic feature of this spectrum is hyperfine splitting due to the isotope of ^{195}Pt ($I=1/2$) with a natural abundance of 33.8%. We have observed also a superhyperfine structure due to interaction with four nearest ^{207}Pb nuclei, which undoubtedly shows that Pt^{3+} substitutes for Ti^{4+}. The spin Hamiltonian parameters of the light-induced Pt^{3+} center in $PbTiO_3$ reported earlier[11] are slightly different from ours (see Table I). The differences are evidently due to the temperature dependence of the g factor, because those measurements have been performed at $T=77$ K. Additionally, Table I includes a superhyperfine splitting constant which was not resolved in Ref. 11. The light-induced Pt^{3+} center appears to be stable up to $T=(70-100)$ K. At higher temperatures the Pt^{3+} ESR spectrum strongly decreases down to its almost total disappearance due to thermal ionization of Pt^{3+} into Pt^{4+}.

Three other light-induced centers are more thermally stable. Their ESR spectra have been observed at low temperatures and could be destroyed by annealing at 150 K. Strong spin-lattice relaxation, being the characteristic feature of these centers, leads to a broadening of the ESR lines beginning from $T=7-10$ K, and finally to their complete disappearance at $T>25-30$ K. In our opinion, these paramagnetic centers are connected with the Ti^{3+} ion. We have denoted them as Ti^{3+}(I), Ti^{3+}(II), and Ti^{3+}(III). The assignment is made on the basis of the g tensors of the centers, having g shifts typical of Ti^{3+} and a hyperfine structure which is resolved at one of the centers [see Fig. 8, Ti(II)]. From our analysis of hyperfine structure follows that it belongs to two titanium ion isotopes: ^{47}Ti ($I=5/2$) and ^{49}Ti ($I=7/2$), having natural abundance of 7.3% and 5.5%, respectively. The values of their magnetic momenta are close to each other.

For Ti^{3+}(I) centers the angular dependences of ESR line positions indicate a very low local symmetry (Fig. 9). The line positions were described by the g-factor values: $g_1=1.965$, $g_2=1.919$, and $g_3=1.848$ with g-tensor axes oriented as shown in Fig. 9. Altogether there are eight such equivalent centers, which are resolvable in the ESR spectra. They differ by the z_2 axis orientations in the (001) plane (the angle $\alpha=60°$, 150°, 240°, and 330°) and by the z_1 axis polar angle ($\beta=60°$ or 120°). Such a low symmetry of the Ti^{3+} (I) center, with none of the g-tensor axes along the

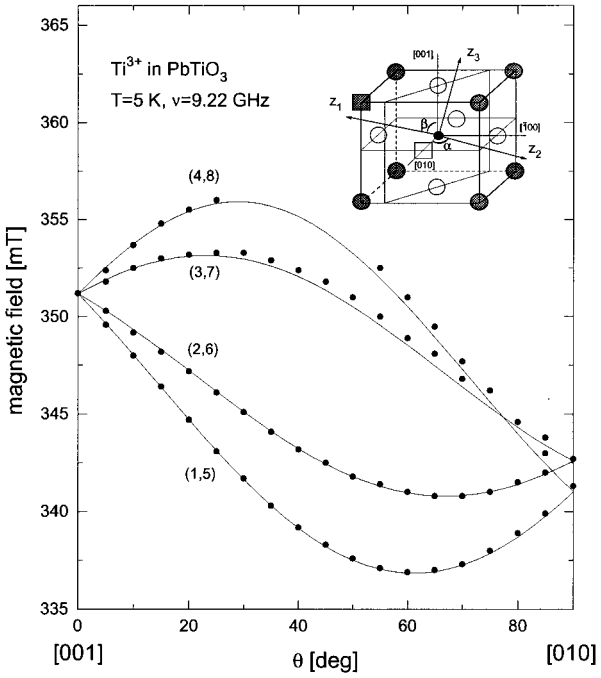

FIG. 9. The angular dependence of resonance fields for the Ti^{3+}-$V_{O(I)}$-*A* [Pb] center, called also Ti^{3+}(I) in the paper (points, experiment; solid lines, theory; the numbers in the brackets numerate the lines of eight equivalent centers). The sketch shows a center model; z_1, z_2, and z_3 are the *g*-tensor principal axes of center 1; α and β are the Euler angles. The ion's designations are the same as in Fig. 1, open and solid squares being an oxygen vacancy and a defect on the Pb site, respectively.

crystal ones, may be ascribed to the presence of some pair-type defect near to the Ti ion. The latter should include the oxygen vacancy $V_{O(I)}$ in the (001) plane, because the axes z_2 of the center lie within the plane containing four oxygen ions, near the Ti-O direction. Note that the number of oxygen vacancies in $PbTiO_3$ is known to be rather high as required for the charge compensation of lead vacancies in the material. On the other hand, deviation of the z_2 axis from the Ti-O direction and the orientations of z_1 and z_3 axes evidence the position of another pair constituent at the Pb site. This may be either a substitution ion on the Pb site or a Pb vacancy (V_{Pb}).

The angular dependence of ESR lines of the Ti^{3+}(II) center exhibits an orthorhombic symmetry, the positions of the lines were described by *g*-factor values: $g_{[001]+\beta}=1.840$, $g_{[110]}=1.855$, and $g_{[1\bar{1}0]+\beta}=1.892$, where the angle $\beta=2°$ means the rotation of the *g*-tensor axes around the [110] direction. Totally four equivalent centers of this type account for the spectrum, they differ by the orientation of two *g*-tensor axes in the (001) plane, the third axis is always directed along [001] + β. This local symmetry of the Ti^{3+} ion may be due to the appearance of a defect on a neighboring Pb site, the latter may be an ion substituted for Pb (*A* [Pb]).

Using the above considerations for Ti^{3+}(I) , one can associate the Ti^{3+}(II) center with the oxygen vacancy along the $\overline{c}$ axis of the crystal ($V_{O(II)}$). Indeed, the oxygen vacancy changes only the value of the tetragonal crystalline field in this case, but orthorhombic *g*-tensor symmetry is connected solely with the Pb site defect.

The light-induced center model is an F_A-center one, i.e., a photoelectron is trapped by the oxygen vacancy, its wave function being smeared on the neighbor ions; it is expected to be localized at one of the two Ti ions next to the oxygen vacancy. Note similar Ti^{3+} centers have been observed in $BaTiO_3$,[17] where the Ba site defect was identified as K^+ or Na^+ ion.

The local electronic levels of these centers used to be shallow donors close to the conduction band edge. The disappearance of the ESR spectrum at $T\geqslant 150$ K may be connected with the thermal ionization of these centers, i.e., their transformation into Ti^{4+}-$V_{O(i)}$-*A* [Pb] (i=I,II). On the contrary, the light beam produces photoelectrons in the conduction band which can be trapped by Ti^{4+}-$V_{O(i)}$-*A* [Pb] centers, transforming them into Ti^{3+}-$V_{O(i)}$-*A* [Pb] with a long enough lifetime at low temperature ($T\leqslant 100$ K).

The Ti^{3+}(III) center has an orthorhombic symmetry like Ti^{3+}(II): $g_{[001]+\beta}=1.954$, $g_{[110]}=1.963$, and $g_{[1\bar{1}0]+\beta}=1.905$. It can be connected with an unknown defect in the Pb site as well. This center is characterized by a strong *g*-tensor anisotropy within the (001) plane, a narrow linewidth ($\Delta B=0.1$ mT) and a weaker temperature dependence of the spin lattice relaxation time compared to that for Ti^{3+}-$V_{O(i)}$-*A* [Pb] centers. Evidently, it is a linear Ti^{3+}-*A* [Pb] defect. This is not an F_A center, its localized states are deeper than those of the F_A center. Indeed, in some $PbTiO_3$ samples we have observed the weak ESR spectrum from the Ti^{3+}(III) centers after heat treatment at $T=800$ K without light illumination. After light illumination of these samples, a sharp increase in the intensity of the Ti^{3+}(III) ESR spectrum is observed. The Ti^{3+}-*A* [Pb] defect evidently arises from the electron transfer to Ti^{4+}, thus, leading to the compensation of the excess charge in the crystal. A similar center was observed in PZT ceramic with *g*-factor values close to those of Ti^{3+}(III).[18] Note that hyperfine structure was not resolved in the Ti^{3+}(I) and Ti^{3+}(III) spectra due to their smaller intensities and more complex shapes.

It is worth to note that in $PbTiO_3$, as in $BaTiO_3$,[17] we have not identified any linear Ti^{3+}-V_O defects. This is evidently connected with the fact that localized electronic levels of the low symmetry centers Ti^{4+}-V_O-*A* [Pb] are deeper than the corresponding levels of the Ti^{4+}-V_O centers and therefore they are the traps for photoelectrons; hence, the Ti^{3+}-V_O centers are not observed .

It was noted earlier that the Ni^{3+} center is sensitive to light illumination. The crystal illumination at $T=10$ K increases the Ni^{3+} ESR line intensity by a factor of about 4. The heating of the crystal up to $T=300$ K leads to line decrease by six to eight times. It can be assumed that the Ni^{3+} local electronic level is also a donor level which is slightly deeper than the Ti^{3+}-V_O-*A* [Pb] donor level.

V. DISCUSSION AND CONCLUSION

In this section we would like to pay attention to peculiarities of the $PbTiO_3$ structure on the basis of the ESR data. It is obvious that we have to begin with looking for a paramagnetic impurity which occupies the same position in the oxygen cage as the Ti^{4+} ion at any temperature. In $BaTiO_3$

Mn^{4+} ions were shown to be such a type of impurities meanwhile Cr^{3+} and Fe^{3+} remain centered in the oxygen octahedron.[12] This centered position may be the consequence of the excess negative charge of these ions in the lattice which repulses negatively charged oxygen.

The desirable information about the paramagnetic center position at any temperature can be obtained on the basis of the analysis of $b_2^0(T)$. To obtain the quantitative data for both Mn^{4+} and Fe^{3+} let us use a superposition Newman model[19] in its truncated form.[20] In accordance with this approach the axial constant b_2^0 can be represented in the form

$$b_2^0=\overline{b_2}(R)\frac{3}{2}\sum_i\left(\frac{R}{R_i}\right)^{t_2}\left(\cos^2\Theta_i-\frac{1}{3}\right). \tag{3}$$

Here, R is the reference point, R_i is the distance between the ith ligand and the paramagnetic ion, θ_i is the angle between R_i and the main ESR axis (symmetry axis of paramagnetic center). The axial model function $\overline{b_2}(R)$ has been derived from unaxial stress experiments for Cr^{3+} in MgO and $SrTiO_3$.[21]

(1) It was found[12,22] that the $\overline{b_2}(R)$ function of Mn^{4+} is almost the same as that of Cr^{3+} substituting for Ti^{4+} in $SrTiO_3$ and $BaTiO_3$. This function is given by[12]

$$\overline{b_2}(R)=-A\left(\frac{R_0}{R}\right)^n+B\left(\frac{R_0}{R}\right)^m, \tag{4}$$

where $A=-11.1\ \mathrm{cm}^{-1}$, $B=-8.48\ \mathrm{cm}^{-1}$, $R_0=0.1905$ nm, $n=10$, and $m=13$.

Using this function, we have calculated the axial parameter b_2^0 of Mn^{4+} for its centered and off-center positions in the oxygen cage. Expression (3) is used with $R=0.207$ nm, $\overline{b_2}(R)=2.2\ \mathrm{cm}^{-1}$, parameter $t_2=0.36$, which is close to that of Cr^{3+} in $BaTiO_3$.[22] In the centered Mn^{4+} position this gives $b_2^0=0.1\ \mathrm{cm}^{-1}$ which is a factor 3 too small compared to the observed value of b_2^0. On the contrary, allowing for Mn^{4+} an off-center displacement d, we have obtained $b_2^0=0.31\ \mathrm{cm}^{-1}$ at $T=290$ K for $d=0.032$ nm taken from x-ray measurements for Ti^{4+} position in $PbTiO_3$.[1] But the most interesting for clearing up both the paramagnetic center model and the lattice structure peculiarities is the analysis of the observed temperature dependence of b_2^0 on the basis of expressions (3) and (4) with the same parameters t_2, R_0, n, etc., which have to be temperature independent. We carried out a calculation of $b_2^0(T)$ at $77\leqslant T\leqslant 700$ K, taking into account the temperature dependence of the lattice constants a and c of $PbTiO_3$ measured in Refs. 23 and 24. The results of the calculations are depicted in Fig. 4 by the solid line which corresponds to the best fit of the measured data. This procedure allows to obtain the temperature dependence of the off-center Mn^{4+} position, which is shown in Fig. 10 by the solid line. In the same figure we also depicted $d(T)$ obtained for Ti^{4+} by different methods: x-ray diffraction,[25] neutron diffraction,[26] and XAFS method.[2] It may be readily seen that ESR data are in rather good agreement with those of neutron diffraction measurements, namely, the Ti^{4+} position changes little up to $T=700$ K, the value of d strongly decreasing only near $T=T_c$ where Ti^{4+} becomes centered. Thus, the ESR data do not confirm recent XAFS results[2] of the relatively off-center Ti^{4+} position in the oxygen cage even at $T>T_c$ (see Fig. 10). Perhaps this discrepancy is connected with an extremely short effective measuring time of the XAFS method (of the order of 10^{-16} sec).

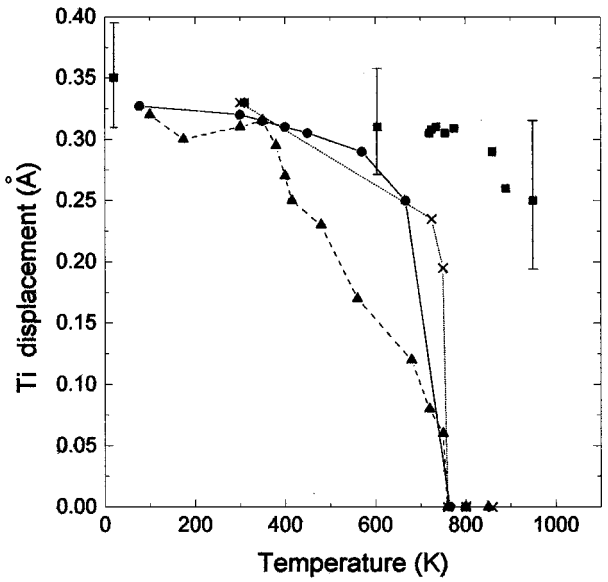

FIG. 10. The temperature dependence of titanium ion displacement in $PbTiO_3$: triangles, crosses, and squares correspond to the data of x-ray diffraction (Ref. 25), neutron diffraction (Ref. 26), and XAFS (Ref. 2), respectively. Solid line and circles depict the temperature dependence of the displacement of Mn^{4+}, which occupies an off-center position in the oxygen cage just as Ti^{4+}.

(2) We carried out the calculation of $b_2^0(T)$ for the Fe^{3+}

TABLE II. Ti^{3+} Centers in $PbTiO_3$ and their ESR spectral parameters.

Ion	T (K)	g	A (10^{-4} cm^{-1})	Remarks
Ti^{3+}(I)	5	g_1: 1.965(1)		Euler angles of g-tensor prin-
(Ti^{3+}-$V_{O(I)}$-A [Pb])		g_2: 1.919(1)		cipal axes: $\alpha=60°$, $\beta=60°$;
		g_3: 1.848(1)		Annealed at 150 K
Ti^{3+}(II)	5	$g_{[001]+\beta}$: 1.840(1)	$A_\parallel$:10(1)	$\beta=2°$
(Ti^{3+}-$V_{O(II)}$-A [Pb])		$g_{[110]}$: 1.855(1)		(rotation around [110])
		$g_{[1\bar{1}0]+\beta}$: 1.892(1)		Annealed at 150 K
Ti^{3+}(III)	10	$g_{[001]+\beta}$: 1.954(1)		$\beta=2°$
(Ti^{3+}-A [Pb])		$g_{[110]}$: 1.963(1)		(rotation around [110])
		$g_{[1\bar{1}0]+\beta}$: 1.905(1)		

ion using relationship (3) with parameters $\overline{b_2}(T)=-0.69$ cm^{-1} and $t_2=8$ which are close to those obtained for this ion in the tetragonal phase of $SrTiO_3$ [see Table I of Ref. 20 with $b_2=-0.57(38)$ cm^{-1}, $t_2=8(1)$]. Performing indicated calculations, we have considered several Fe^{3+} paramagnetic center models, namely, with and without oxygen vacancy in the ion's nearest neighbor position (the excess charge of Fe^{3+} has to be compensated) as well as the off-center or the centered position of Fe^{3+} in the oxygen cage. An agreement with experimental data (corresponding to the solid curve in Fig. 6) was obtained only in the model with Fe^{3+} in the center of the oxygen octahedron without an oxygen vacancy in the nearest neighbor. Note that the temperature dependence of b_2^0 is almost determined by the temperature dependence of the lattice constants $a(T)$ and $c(T)$.

(3) From the observation and the analysis of the ESR spectra of nominally pure single crystal $PbTiO_3$ of high quality (before and after light illumination) several paramagnetic centers: Mn^{4+}, Fe^{3+}, Ni^{3+}, Pt^{3+}, Ti^{3+}-$V_{O(i)}$-*A* [Pb], Ti^{3+}-*A* [Pb] — the last four centers being induced by light — may be identified. Mn^{4+} is shown to be a good paramagnetic probe for the investigation of lattice distortions in a relatively wide temperature range up to $T\approx 800$ K including the phase transition region. However, the Mn^{4+} ESR spectrum in $BaTiO_3$ is observed only in the low-temperature rhombohedral phase because of dynamic peculiarities of this material (existence of the relaxation mode[12]). Thus, $PbTiO_3$ dynamics seems to be different from that of $BaTiO_3$. The off-center displacements of Ti^{4+} ions at $T>T_c$ shown recently by the XAFS method are not confirmed by the ESR data. As the magnetic Mn^{4+} ions follow the cooperative motion of Ti^{4+} ions which contribute strongly to the material ferroelectric properties, a high degree of magnetoelectric coupling can be assumed in the mixed perovskite $PbTi_{1-x}Mn_xO_3$ crystal. This material may be of considerable interest due to a possible coexistence of magnetic and electric ordering at the same temperature.

The series of light-sensitive centers discovered in $PbTiO_3$ (Ni^{3+}, Ti^{3+}-$V_{O(i)}$-*A* [Pb] and Ti^{3+}-*A* [Pb]) can be of great importance for the analysis of any photoinduced phenomena, such as photocurrent, photoluminescence, etc. The observation of these phenomena in the $PbTiO_3$ single crystal illuminated by light is extremely desirable. Note that in our opinion, the light-induced Ti^{3+} centers should also be present in the photorefractive PLZT ceramic. As the Ti^{3+}-$V_{O(i)}$-*A* [Pb] complexes are F_A centers, their role in the light-induced charge transport may be essential. A recently observed light-induced Ti^{3+} center in PLZT (Ref. 27) might be such an F_A center. To identify Ti^{3+} centers in both $PbTiO_3$ and PLZT in more detail, complex measurements of ESR, optical absorption and other photoinduced phenomena should be performed.

[1] G. Shirane, R. Pepinsky, and B. C. Frazer, Acta. Crystallogr. **9**, 131 (1956).

[2] N. Sicron, B. Ravel, Y. Yacoby, E. A. Stern, F. Dogan, and J. J. Rehr, Phys. Rev. B **50**, 13 168 (1994).

[3] M. D. Glinchuk, V. V. Laguta, I. P. Bykov, J. Rosa, and L. Jastrabík, Chem. Phys. Lett. **232**, 232 (1995).

[4] E. Possenriede, P. Jacobs, and O. F. Schirmer, J. Phys. Condens. Matter **4**, 4719 (1992).

[5] D. J. A. Gainon, Phys. Rev. **134**, 1300 (1964).

[6] O. Lewis and G. Wessel, Phys. Rev. B **13**, 2742 (1976).

[7] R. G. Pontin, E.F. Slade, and D.J.E Ingra, J. Phys. C **2**, 1146 (1969).

[8] T. Q. Chien, W. Windsch, and B. Milsch, *Ferroelectrizität 86* (Halle, BRD, 1987), p. 152.

[9] R. Heidler, W. Windsch, R. Bottcher, and C. Klimm, *Ferroelectrizität 89* (Halle, BRD, 1990), p. 142.

[10] D. J. Keeble, Z. Li, and E. H. Poindexter, J. Phys. Condens. Matter **7**, 6327 (1995).

[11] W. L. Warren, B. A. Tuttle, B. N. Sun, Y. Huang, and D. A. Payne, Appl. Phys. Lett. **62**, 146 (1993).

[12] K. A. Müller, W. Berlinger, and K. W. Blazey, Solid State Commun. **61**, 21 (1987).

[13] K. A. Müller, Phys. Rev. Lett. **2**, 341 (1959).

[14] M. D. Glinchuk and I. P Bykov, Phase Trans. **40**, 1 (1992).

[15] A. P. Pechenyi, M. D. Glinchuk, T. V. Antimirova, and W. Kleeman, Phys. Status Solidi B **174**, 325 (1992).

[16] J. E. Wertz and J. R. Bolton, *Electronic Spin Resonance* (McGraw-Hill, New York, 1972).

[17] R. Schafschwerdt, O. F. Schirmer, H. Krose, and Th. W. Kool, Ferroelectrics (to be published).

[18] I. P. Bykov, M. D. Glinchuk, V. G. Grachov, Y. V. Martynov, and Vl. Skorokhod, Fiz. Tverd. Tela, **33**, 3459 (1991) [Sov. Phys. Solid State **33**, 1943 (1991)].

[19] D. I. Newman and W. Urban, Adv. Phys. **24**, 793 (1975).

[20] E. Siegel and K. A. Müller, Phys. Rev. B **19**, 109 (1979).

[21] W. Berlinger and K. A. Müller, Rev. Sci. Instrum. **48**, 1161 (1977).

[22] K. A. Müller and W. Berlinger, Phys. Rev. B **32**, 5837 (1985).

[23] G. Shirane and S. Hoshino, J. Phys. Soc. Jpn. **6**, 265 (1951).

[24] J. Kobayashi, Ferroelektrics **37**, 571 (1981).

[25] M. F. Kaprianov, S. M. Zaitsev, E. S. Gagarina, and E. G. Fesenko, Phase Trans. **4**, 55 (1983).

[26] R. J. Nelmes, R. O. Piltz, W. F. Kuhs, Z. Tun, and R. Restori, Ferroelectrics **108**, 165 (1990).

[27] W. L. Warren, C. H. Seager, D. Dimos, and E. J. Friebele, Appl. Phys. Lett. **61**, 2530 (1992).